

Research on the calculation modeling and method of laser fuse echo power considering the influence of atmospheric suspended particles

XIAOQIAN ZHANG*, HANSHAN LI, JUNCHAI GAO

School of Electronic and Information Engineering, Xi'an Technological University, Xi'an, 710021, China

The presence of suspended particles in the atmospheric environment has a significant impact on the detection performance of pulse laser fuse detection systems. Based on the transmission characteristics of pulse laser fuse in particle atmosphere and Mie scattering theory, a particle backscattering model is established, and the necessary conditions for the successful reception of laser beam by photoelectric receiver are determined. By taking into account the transmission time and frequency of the backscattering photon as well as the photon weight after the collision between the photon and the particle, a multi-factor calculation model of laser emission power is constructed, and the mathematical model of the echo power of the system receiving ground targets is derived. Through simulation experiments, the paper obtains the echo characteristics of pulse laser in various detection scenarios. An analysis is conducted on the backscattering characteristics of smoke particles under different laser pulse widths, mass concentrations of smoke particles, and missile-target intersection distances, revealing the impact patterns of these conditions on scattering occurrences and echo results. These research findings provide a basis for exploring methods to enhance the detection performance of laser fuses in complex environments.

(Received October 25, 2023; accepted February 9, 2024)

Keywords: Laser fuse, Detection performance, Backscattering, Echo characteristics

1. Introduction

The widespread application of laser fuses in precision-guided munitions can be attributed to the excellent directional and good monochromatic properties of laser beams. However, in the battlefield environment, suspended particles such as smoke and fog in the atmosphere act as optoelectronic interference sources, which results in the degradation or even failure of the detection performance of laser fuses [1-4]. Addressing this issue and enhancing the detection performance of laser fuses in the presence of particle interference remain crucial challenges.

Currently, the pulse broadening characteristics of backscattered echoes caused by clouds and fog on laser fuses were studied by Zhang et al. [5-6]. The effects of laser fuse structure, laser signal transmission form, and distance between laser fuse and cloud/fog boundary were analyzed. However, relying solely on echo broadening information is insufficient for distinguishing particle echoes from ground target echoes. A detection model for pulse laser fuses in clouds and fog was established by Wang et al. [7-8]. The echo characteristics when targets exist in clouds and fog were studied, and the appearance pattern of the double-peak phenomenon in echoes under specific conditions was analyzed. At the same time, several solutions have been proposed by researchers, encompassing ultra-narrow pulse detection technology, dual-wavelength laser detection technology, and

polarization detection technology [9-12]. Among them, ultra narrow pulse technology mitigates interference by reducing the backscattering intensity in clouds and fog. Dual-wavelength laser detection technology distinguishes interference by exploiting the variations in laser scattering characteristics at different wavelengths in clouds and fog. Polarization detection technology enhances the accuracy of target detection and recognition by augmenting target information. These detection technologies leverage distinctions in characteristics between the backscattered echoes of aerosols and target-reflected echoes to identify and eliminate clutter interference. The characteristics of backscattered echoes of aerosols are closely tied to their scattering properties, such as the number of scattering within aerosols. A more profound analysis of these characteristics is facilitated by examining the scattering characteristics of backscattered aerosol echoes. The composite detection technology, which introduces a detection system that is insensitive to cloud and fog interference, has been employed to improve the anti-interference capability. In reference [13], a study on laser and radio composite detection technology was conducted, and a Frequency-Modulated Continuous Wave (FMCW) laser and radio composite detection technology was proposed. Based on the frequency-differential signal obtained through the laser and radio detection methods, a digital signal processing algorithm was applied for comprehensive assessment and processing, achieving the

goal of resisting interference from cloud and fog and enhancing detection accuracy, which can effectively address the challenges of laser detection technology's anti-interference capability against cloud, smoke, rain, and snow interference. In reference [14], a laser cloud transmission model was established and simulated to analyze the characteristics of the backscattering laser echoes, including the number of scattering times, behind the cloud. Additionally, several factors, such as inherent parameters of the laser fuse detection system, changes in echo signal waveform, noise, target reflection characteristics, and detection distance, will affect the detection capability of the laser fuse [15-16]. Additionally, the study marks the inaugural reporting of the oxidative potential of water-soluble organic matter related to the chromophoric substances in PM_{2.5} over Xi'an, China; and the discovery can offer insights into predicting the oxidative potentials of light-absorbing organic aerosols based on their optical properties [17]. Due to the heating effect of Black Carbon, which can increase the ground-level temperature, the lower boundary of the inversion layer has been elevated, which further mitigates and aggravates both haze and O₃ pollution. In the work by Wang et al. [18], observational evidence was explored, highlighting the dual roles of BC in the megacity of eastern China: enhancing O₃ and decreasing PM_{2.5} pollution. Tan et al. [19] delved into the interaction between black carbon and the planetary boundary layer in the Yangtze River Delta spanning from 2015 to 2020: addressing the question of why O₃ didn't decline so significantly as PM_{2.5}, this study conducted a long-term observation on black carbon and utilized the observational data for other air pollutants (PM_{2.5}, PM₁₀, NO₂, SO₂, CO and O₃), meteorological elements, and vertical sounding data of the Planetary Boundary Layer in Nanjing. The connection between wildfires and climate have been extensively studied, as demonstrated by reference [20], showcasing the primacy of synoptic-scale feedback in driving extreme fires in Mediterranean and monsoon climate regimes in the West Coast of the United States and Southeastern Asia, the result indicated that the intricate interactions among wildfires, smoke, and weather form a positive feedback loop that substantially amplifies air pollution exposure.

This paper takes the battlefield environment as the testing background, characterized by the suspension of numerous particles like dust and smoke. Based on this, this study investigates the differences in the echo characteristics between suspended particles and ground targets in the atmospheric environment to identify the source of the laser fuse echo and eliminate the particle interference, thus enhancing the detection ability of the laser fuse in a complex environment. Meanwhile, utilizing the Mie scattering theory and Monte Carlo method, the motion trajectory of the laser photon cluster emitted by the

laser in a complex environment was analyzed, and integrated with the backscattering effect of particles in the missile-target interception state, a laser emission model, a laser transmission model in the environment, and a laser reception model were established. Taking into account the backscattering characteristics of the laser in the atmospheric environment, the transmission time and frequency of the backscattered photons from particle, along with the photon weight after colliding with particles, were introduced to establish the laser emission power model for the backscattering of the laser through suspended particles in the atmospheric environment. By combining the target echo power calculation function in the missile-target intersection state, the mathematical model for the received target echo power of the laser fuse detection system under complex atmospheric environment was derived. The main work and contributions of this paper are as follows:

(1) Considering the backscattering effect of particles in the atmospheric environment, the laser emission model, the laser transmission model in the environment and the laser reception model are established to provide the transmission characteristic model for analyzing the target echo signal.

(2) The calculation model of laser emission power after backscattering is constructed by introducing the characteristics of particle backscattering echo photons and the characteristics of mutual collision, which provides accurate information on laser emission power in the particle environment.

(3) The calculation method of the echo power of the system receiving the ground target under the intersection state of the missile and the ground target is studied, which lays a foundation for the reliable detection of the laser pulse fuse in other atmospheric environments.

2. The laser fuse detection principle

The performance of weapons using laser as a detection method is significantly impacted by suspended particles such as clouds, smoke, and dust in the atmospheric environment, particularly the interference echo signals generated by the backward scattering of smoke particles suspended in the missile explosive environments, which lead to false alarms or misjudgments of laser fuse and ultimately affect the detection performance of the system. Additionally, suspended particles exhibit unique light scattering characteristics in the air due to their properties and laser wavelength [21-22], and therefore, the emission, transmission, and reception models of lasers in the atmospheric environment must be considered when investigating the echo characteristics of ground targets detected by laser fuse. The schematic diagram of laser fuse detection principle is illustrated in Fig. 1.

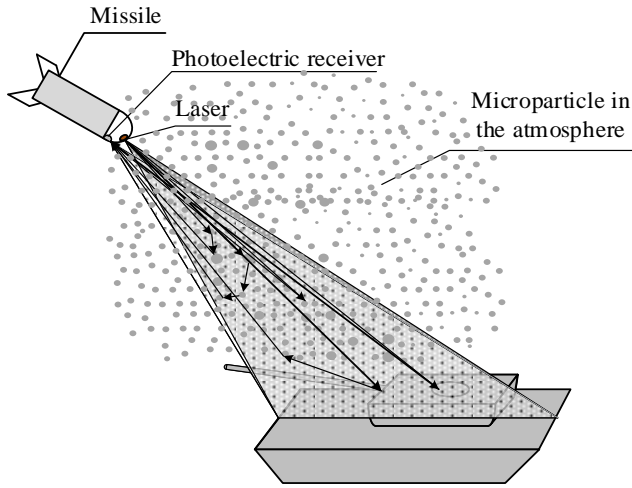


Fig. 1. Schematic diagram of the laser fuse detection principle

In Fig. 1, the missile comprises guidance module, warhead, laser fuse, fuel tank, etc. Among them, the laser fuse primarily consists of a laser detection module located at the front end of the missile and an initiation control module. The missile aims and approaches the target under the control of the guidance module. The laser detection module emits a pulse laser beam with a certain frequency and angle to detect the target. The receiving system captures the reflected light from the target and converts it into an electrical signal. The detonation control module located at the bottom of the warhead, after distance discrimination, detonates the center detonator at the optimal detonation height [23], warhead fragments hit the target at a specific flying azimuth angle under the detonation effect of the warhead charge. This paper investigates the pulse laser fuse as a leading laser fuse, featuring a certain forward inclination angle to form a laser detection field. This ensures target recognition and optimal detonation of the warhead at the appropriate time under the intersection state.

3. Modeling of laser backscattering in atmospheric environment

The laser fuse detection system decomposes the laser emitted by the pulse laser source into a photon group, serving as the detection unit. The trajectory of this photon group in the environment undergoes analysis using Mie scattering theory and Monte Carlo method. Integrated with the scattering effect of the environment's particles in the missile-target intersection state, the target echo energy is obtained in the laser fuse receiving optical module. According to the formation process of the target echo, it's crucial to establish models for laser emission, laser propagation in the environment, and laser reception.

To reduce photon divergence, the photons emitted by the laser source undergo shaping by the optical system of emitting end before entering the atmospheric environment. The optical system, featuring a plano-convex lens, utilizes

the two refractions occurring as photons pass through it to reduce the divergence angle of photon movement direction. The laser beam is emitted into the atmospheric environment for detection through the optical system. The number of photons emitted from each position at the laser beam waist, acting as the photon emission point, follows a Gaussian distribution [24-26], and the direction of photon transmission is adjusted by the optical shaping system of emitting end. The position of photon emission at the time of emission can be expressed as:

$$\begin{cases} x_{st} = \omega_0 \eta_1 \\ y_{st} = \omega_0 \eta_2 \\ z_{st} = 0 \end{cases} \quad (1)$$

where, ω_0 is the waist radius of the laser beam, $\omega_0 = (\lambda \kappa / \pi)^{1/2}$; λ is the wavelength of the laser; κ is the Rayleigh length; η_1 and η_2 are random numbers of the standard normal distribution[27]. The direction of the photon at the moment of emission is:

$$\begin{cases} u_{sx} = \sin \alpha_0 \cos \beta_0 \\ u_{sy} = \sin \alpha_0 \sin \beta_0 \\ u_{sz} = \cos \alpha_0 \end{cases} \quad (2)$$

where, α_0 is the zenith angle of the photon emission direction, $\alpha_0 = [(\alpha'/2) \cdot \eta_3]$; α' is the divergence angle of the laser emission beam; η_3 is a standard normal distribution random number; β_0 is the azimuth angle of the photon emission direction, $\beta_0 = 2\pi \cdot \eta_4$; and η_4 is uniform distribution random numbers on the interval [0,1].

As photons emitted from the laser permeate the atmospheric environment, their interaction with suspended particles, like clouds, fog, and smoke, induces photon scattering. Additionally, the energy of the photons also undergoes attenuation during the transmission and movement. The size of smoke particles is determined by sampling in accordance with the particle size distribution [28-30], and is analyzed by least-squares regression and significance testing. The particle size distribution function of smoke particles is obtained as:

$$N(r) = ar^\varepsilon \exp(-br^\chi) \quad (3)$$

where, r is the particle diameter; a , b , ε and χ are distribution parameters.

After colliding with smoke particles, photons continue to move in a new direction and their energy is attenuated.

The alteration in photon energy post-scattering with smoke particles can be expressed as:

$$E_{s,s} = \frac{Q_s}{Q_e} E_s \quad (4)$$

where, E_{ss} and E_{st} are represented the energy of photons before and after scattering, respectively; Q_s is the scattering efficiency factor of smoke particles; Q_e is the extinction efficiency factor of smoke particles; and $\varpi = \frac{Q_s}{Q_e}$ is the weight of photons after collision with smoke particles, determined by the single-scattering albedo [31], expressed as:

$$Q_s = \frac{2}{\tau^2} \sum_{i=1}^{\infty} (2i+1)(|a_i|^2 + |b_i|^2) \quad (5)$$

$$Q_e = \frac{2}{\tau^2} \sum_{i=1}^{\infty} (2i+1) \text{Re}(a_i + b_i) \quad (6)$$

where, τ is the size parameter of the smoke particle; a_i and b_i are the Mie scattering coefficients.

According to the scattering mean free path, the calculation function for determining the distance traveled by photons between two collisions with smoke particles is:

$$\Delta S = -\frac{\ln \zeta_1}{\mu_t} \quad (7)$$

where, ζ_1 is a uniformly distributed random number within [0,1] range; μ_t is the particle attenuation coefficient, $\mu_t = \sum_{j=1}^l \frac{3Q_e}{4\rho r_j} C(r_j)$; ρ is the density of smoke particles; and $C(r_j)$ is the mass concentration of smoke particles [32].

The scattering direction of photons colliding with smoke particles is determined by sampling the Mie scattering phase function, expressed as:

$$P(\alpha) = \frac{|S_1(\alpha)|^2 + |S_2(\alpha)|^2}{\sum_{i=1}^{\infty} (2i+1)(|a_i|^2 + |b_i|^2)} \quad (8)$$

where, $S_1(\alpha)$ and $S_2(\alpha)$ are the scattering amplitude functions; α is the scattering zenith angle [33].

Assuming the photon moves in the field of view direction of the laser fuse photoelectric receiver after leaving the atmospheric environment, the photon may be

received by the photoelectric receiver, contributing to the target echo energy obtained by the system. At this point, the position of the photon reaching the plane of the photoelectric receiver is given by:

$$\begin{cases} x_r = x_{sl} - u_{xsl} \frac{z_{sl}}{u_{zsl}} \\ y_r = y_{sl} - u_{ysl} \frac{z_{sl}}{u_{zsl}} \\ z_r = 0 \end{cases} \quad (9)$$

where, (x_{sl}, y_{sl}, z_{sl}) represents the position where the photon scatters or reflects for the last time before leaving the atmospheric environment; $(u_{xsl}, u_{ysl}, u_{zsl})$ represents the direction of the photon at the last scatter or reflection. At this moment, the incident angle of the photon can be expressed as:

$$\alpha_{in} = \arcsin(u_{xsl}^2 + u_{ysl}^2) \quad (10)$$

If the position's arrival position falls within the window of the photoelectric receiver, and the incident angle of the photon lies within the field of view angle of the laser fuse photoelectric receiver, then the photon is successfully received by the photoelectric receiver. This can be expressed as:

$$\begin{cases} (x_r - d_{tr})^2 + y_r^2 \leq R_o^2 \\ \alpha_{in} \leq \frac{\alpha_{view}}{2} \end{cases} \quad (11)$$

where, d_{tr} represents the distance between the transmitting and receiving axis of the laser fuse; R_o represents the radius of the optical lens at the receiving module; α_{view} represents the field of view angle of the photoelectric receiver [34].

If both conditions are satisfied, the photon is successfully received, and the transmission time and frequency of the backscattered photon from the smoke particles are given by:

$$\begin{cases} t = \frac{L}{c} \\ f_{rec} = f_{trans} + \frac{2v}{\lambda} \cos \tilde{\theta} \end{cases} \quad (12)$$

where, L represents the displacement of photons during transmission; c represents the speed of light; f_{trans} represents the frequency of photons emitted; v represents the speed of smoke particles in the atmospheric environment; $\tilde{\theta}$ represents the angle between the

direction of particle movement and the direction of photon flight in the atmospheric environment [35].

4. Target echo power calculation model

In the study of the laser fuse detection system, the single-beam laser is utilized for ground targets detection, employing the line scanning method throughout the detection process. The detection schematic diagram of the single-beam laser is presented in Fig. 2. In Fig. 2, O represents the center position of the ground target; γ_1 is the angle between the laser beam detecting the front of the target and the axis of the missile; γ_2 is the angle between the laser beam detecting the rear of the target and the axis of the missile; δ is the angle between the axis of the missile and the ground target movement direction; ψ is the angle between the direction of the missile's axis and the direction of gravity; L' is the distance from the intersection point between the missile's axis and the target central's axis to the rear of the target; s_t is the length of the ground target.

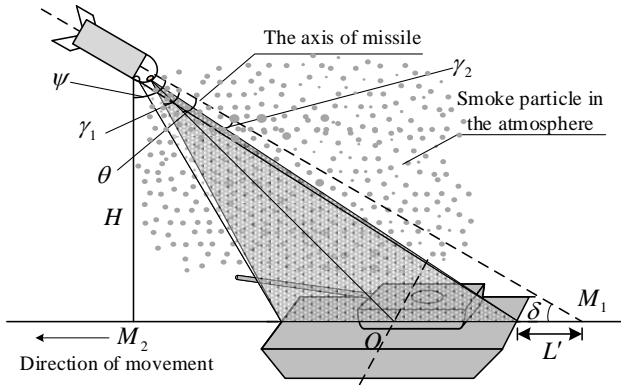


Fig. 2. Illustration of single-pulse laser fuse target detection

To ensure the detection of the ground target by the laser fuse, the target detection is carried out within a detection area $W = \{\gamma_1, \gamma_2\}$. Based on the geometric relationship in Fig. 2, the following equation can be obtained:

$$\gamma_1 = \psi - \arctan \frac{H \cdot \cot \delta - L' - s_t}{H} \quad (13)$$

$$\gamma_2 = \psi - \arctan \frac{H \cdot \cot \delta - L'}{H} \quad (14)$$

The missile intersects with the ground target at a specific elevation angle, taking into account the angle between the normal of the target's surface and the emitted laser beam. Assuming that the ground target's surface

exhibits diffuse reflection characteristics [36], the target echo power received by the laser fuse detection system when the missile is not rolling is expressed as follows:

$$P_{re} = P_t \frac{A_r \tau_r \tau_t \chi \mathcal{G} \cos(\psi - \theta)}{\pi R^2} \quad (15)$$

where, P_{re} is the target echo power; P_t is the laser emission power; A_r is the effective receiving aperture area of the optical lens, $A_r = \pi D^2/4$; D is the receiving aperture of the optical lens; τ_r is the penetration rate of the receiving optical system; τ_t is the penetration rate of the emission optical system, χ is the reflectivity of the ground target's surface; \mathcal{G} is the two-way atmospheric penetration rate, related to the laser wavelength and atmospheric visibility; θ is the pulse laser beam emission angle; and R is the distance between the laser fuse and the target.

In accordance with the geometric relationship between the distance of the laser fuse and the target and the detonation height of the fuse shown in Fig. 2, the distance of the laser fuse and the target can be obtained as:

$$R = H / \cos(\psi - \theta) \quad (16)$$

Considering the backscatter characteristics of laser in the atmospheric environment, including the transmission time and frequency of backscattered photons, as well as the weight of photons colliding with particles, the laser emission power model $P'_t(t, \varpi, f_{rec})$ was established. This model considers the effects of smoke particles on laser emission power after scattering. Combining with formula (15), the expression for the received echo power of a ground target by the laser fuse detection system in a complex atmospheric environment can be obtained as follows:

$$P_{re} = P'_t(t, \varpi, f_{rec}) \frac{\tau_r \tau_t \chi \mathcal{G} D^2 \cos^3(\psi - \theta)}{4H^2} \quad (17)$$

The magnitude of the target echo power diminishes with an increase in the laser beam emission angle and the detection height; at the same time, it is also affected by the backscattering of smoke particles in the atmospheric environment, along with factors such as the scattering efficiency factor and extinction efficiency factor of the smoke particles, leading to the attenuation of photon energy.

The target echo power received by the photoelectric receiver of the system undergoes processing through a signal conversion module, and the final output signal of the system is expressed in the form of a voltage signal, which can be represented as:

$$V_{echo} = \delta_i \cdot A_v \cdot P'_i(t, \varpi, f_{rec}) \frac{\tau_r \tau_t \chi \mathcal{G} D^2 \cos^3(\psi - \theta)}{4H^2} \quad (18)$$

where, δ_i is the current sensitivity of the photoelectric receiver; A_v is the voltage amplification factor of the amplifier circuit in the signal conversion and processing module.

When no targets traverse the test area of laser fuse detection system, the output signal of the photoelectric receiver in the system mainly originates from environmental noise outside the photoelectric receiver. In this scenario, the photoelectric receiver fails to detect the target echo signal. The probability is defined as the false alarm probability of the system when the current noise exceeds the threshold. When the target traverses the test area, the photoelectric receiver in the system detects not only the environmental noise but also the target echo signal. At this time, the system output signal contains the target echo signal and the noise signal superimposed on it. The probability is defined as the detection probability of the system when the peak value of the system output signal surpasses the threshold. These two indicators characterize the detection performance of the system and are expressed by the formulas (19) and (20), respectively.

$$P_{FA} = \frac{1}{2} \operatorname{erfc} \left(\frac{V_{thre}}{\sqrt{2} \bar{V}_n} \right) \quad (19)$$

$$P_D = \frac{1}{2} \operatorname{erfc} \left(\frac{V_{thre} - V_{echo}}{\sqrt{2} \bar{V}_{en}} \right) \quad (20)$$

where, V_{thre} is the threshold voltage set by the system, which is determined when the environment is relatively stable; When the environment detected by the laser fuse remains relatively stable, and the amplitude of the external noise detected by the system exhibits minimal variation, two times of the maximum noise value is selected as the detection threshold of the system. In cases where significant interference exists in the external environment, and substantial environment changes occur over time, the detection threshold of the system is set slightly below twice of the system noise. At the same time, the system noise changes caused by environmental changes mean that the detection threshold of the system also needs to change with the noise, so as to reduce the unnecessary false triggering of the system as much as possible. To keep the false alarm probability and detection probability of the system low, the threshold set by the system cannot be too low. $\operatorname{erfc}(\cdot)$ is the complementary error function; \bar{V}_n is the root mean square of the noise voltage; \bar{V}_{en} is the root mean square of the noise voltage when there is an echo signal. If the external environment undergoes significant changes, the threshold voltage can be adjusted appropriately to stabilize the system's detection

performance.

5. Simulation results and analysis

In the laser fuse detection system, the wavelength of pulse laser is 915 nm, and the width of the pulse laser is modulated within the range of 10 ns to 100 ns. The laser beam divergence angle is 5 mrad, with a diameter of the receiving optical system measuring 9.4 mm. The receiving field of view angle is 20 mrad, and the distance between the receiving and transmitting optical axis is 42 mm. The particle size range of the atmospheric environment is 0.1 μm - 100 μm , with the refractive index of the particles denoted as $1.329 - 4.91 \times 10^{-7}$. The reflectivity of target's surface is about 0.3.

When the laser fuse fails to detect the ground target, the system obtains the backscattered waveform of the smoke particles under varying laser pulse widths of 10 ns, 20 ns, 50 ns, and 100 ns, as depicted in Fig. 3. Conversely, when the laser fuse detects the ground target, under identical laser pulse width conditions, Fig. 4 shows the mixed backscattered waveform of the target and the smoke particles. In Figs. 3 and 4, the horizontal axis represents a time series with the laser emission time as the zero point, and the vertical axis represents the normalized echo intensity sequence based on the peak power of the emission laser.

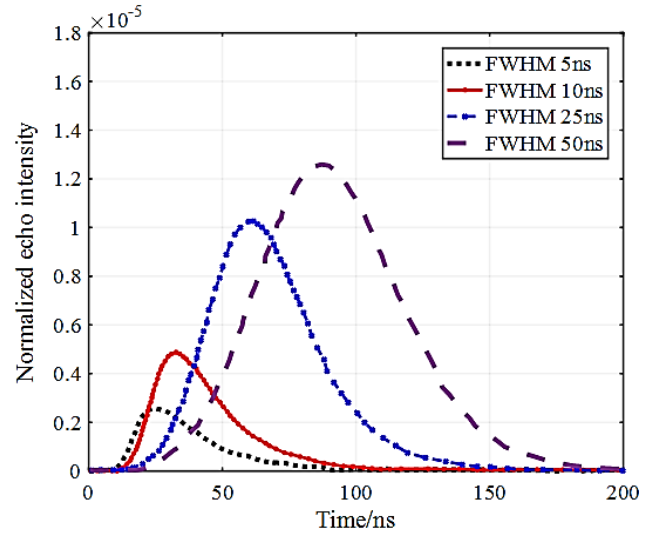


Fig. 3. The backscattered waveforms of smoke particles obtained by the system under different laser pulse width conditions (color online)

From Fig. 3, it is evident that the backscattered echo waveform from the smoke particles in the pulse laser fuse remains a pulse signal, but it has undergone certain changes. In comparison with the emission laser waveform,

the smoke particles backscattered echo waveform is distorted and no longer exhibits a pulse waveform that is entirely symmetrical about the peak. The variation is primarily manifested in the proportion of the rising and falling edges of the echo waveform in the echo broadening, with the falling edge occupying a larger proportion and presenting a non-symmetrical pulse waveform characterized by a steep rising edge and a gentle falling edge.

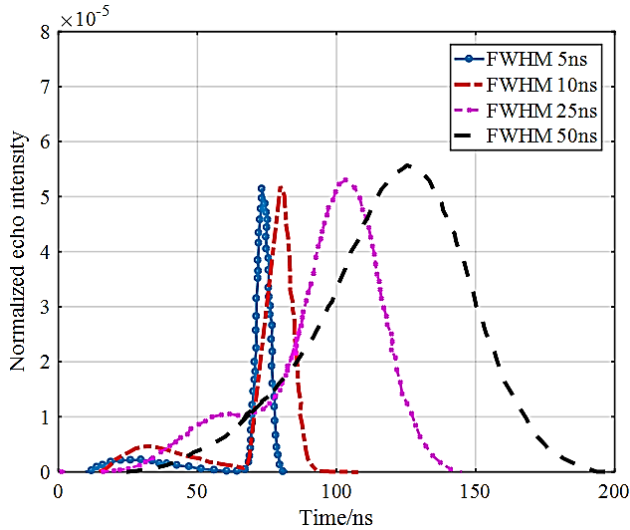


Fig. 4. The mixed echo waveform of target and smoke particles (color online)

In Fig. 4, when the laser pulse width is narrow, two distinct peaks emerge in the laser echo waveform, with the first peak mainly caused by smoke particle backscatter and the second peak mainly caused by target echo. As the laser pulse width increases, the smoke particle backscatter peak gradually diminishes and becomes less prominent in the waveform, resulting in a single peak in the laser echo waveform. The results suggest that the probability of multiple peaks in the laser echo waveform is greater for narrow pulse width lasers than for wide pulse width lasers. Therefore, in the laser fuse detection system, narrow pulse width lasers are more effective in separating particle backscatter from target echo.

Under the condition of constant intersection angle and distance between the missile and target, the variation curve of target echo power with different mass concentrations of smoke particles in the atmospheric environment is calculated, and the results are shown in Fig. 5.

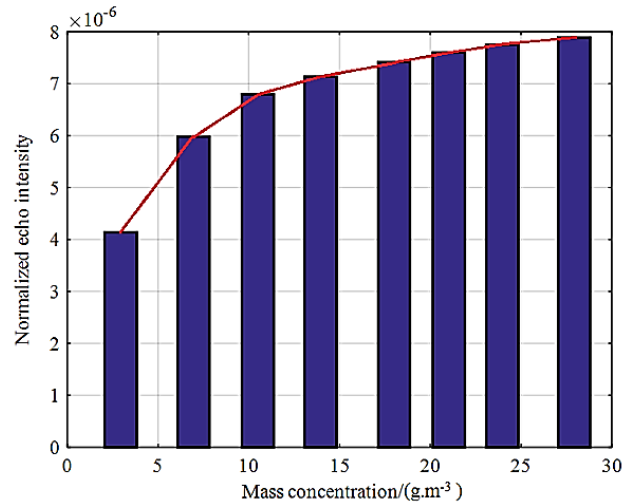


Fig. 5. The variation curve of the target echo power under different particle mass concentration conditions (color online)

Fig. 5 shows that the pulse laser target echo intensity is proportional to the mass concentration, and it is a nonlinear change. This is mainly because the mass concentration of smoke particles increases to a certain extent, and the reflective impact of smoke particles on laser beam photons has reached a maximum, causing the echo intensity no longer increase rapidly with the mass concentration of smoke particles, especially under the conditions with high mass concentration of smoke particles, the speed of echo intensity increase becomes very slow. Based on the testing platform and environment of this paper, the test results were obtained as follows: when the mass concentration of smoke particles exceeds $15 \text{ g}\cdot\text{m}^{-3}$, the change in echo intensity gradually decelerates; when the mass concentration of smoke particles surpasses $26 \text{ g}\cdot\text{m}^{-3}$, the echo intensity ceases to increase with the increase of mass concentration.

The variation curves of echo intensity and mass concentrations of smoke particles are depicted in Fig. 6 at different missile-target intersection distances of 5 m, 6 m, 8 m, and 10 m. The results from Fig. 6 suggest that, with a constant mass concentration, there exists an inverse relationship between the missile-target intersection distance and the echo intensity; the farther the missile-target intersection distance, the smaller the echo intensity. Additionally, as the mass concentration decreases, the declining trend of echo intensity gradually slows down.

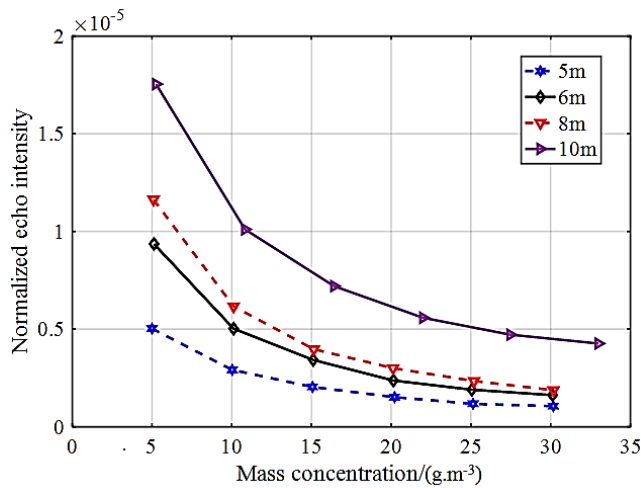


Fig. 6. The variation curves of echo intensity and mass concentrations (color online)

Due to the influence of smoke particles on the backward scattering of laser beams, Fig. 7 illustrates the distribution of the echo intensity of the laser echo scattered by smoke particles as the scattering times. Fig. 7(a) shows the distribution of the echo intensity under the condition of different mass concentrations, while Fig. 7(b) depicts the distribution of the echo intensity under the condition of different missile-target intersection distances. In Fig. 7(a), when the mass concentration of smoke particles is 14 g/m^3 , the energy proportions of the backscattered echo with scattering times ranging from 1 to 5 are 47.41%, 25.74%, 12.09%, 6.02%, and 2.65%, showing a significant attenuation trend of echo energy with increasing scattering times. With the variation of mass concentration of smoke particles, the energy of echo exhibits the same trend. When the mass concentration of smoke particles is 2, 8, 14, and 20 g/m^3 , the scattering times of the backscattered echo from the smoke particles are 2, 3, 3, and 4 times, respectively. This indicates that the total scattering times of the backscattered echo from the smoke particles are proportional to the mass concentration of smoke particles. In Fig. 7(b), the laser echo energy under different missile-target intersection distances exhibits a decay trend with increasing scattering times. When the missile-target intersection distances are 1, 3, 5, and 8 m, the scattering times of the backscattered laser echo from the smoke particles are 4, 3, 3, and 3 times, respectively. This indicates that the total scattering times of the backscattered echo from the smoke particles are inversely proportional to the missile-target intersection distance.

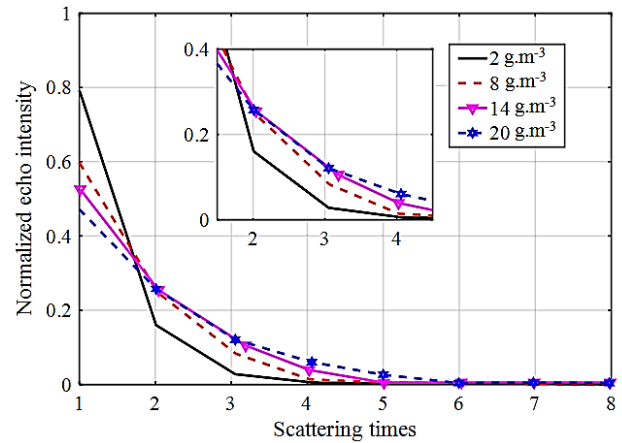


Fig. 7(a). The distribution of the echo intensity under the condition of different mass concentrations (color online)

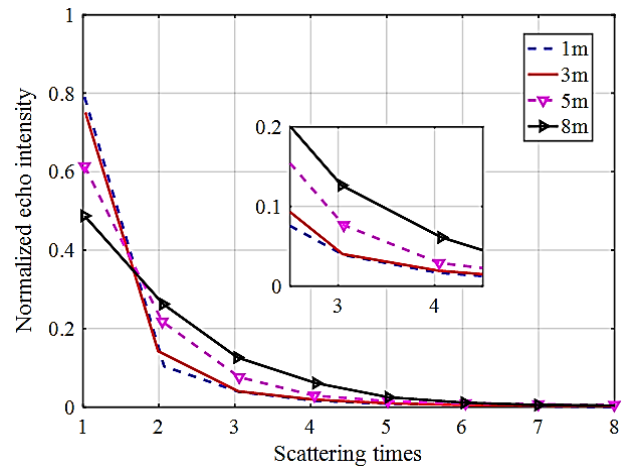


Fig. 7(b). The distribution of the echo intensity under the condition of different missile-target intersection distances (color online)

In the case where the mass concentration of smoke particles is 8 g/m^3 and the missile-target intersection distance is 1 m, the time-domain waveform and the width curve of the same scattering echo within the backscattered echo from the smoke particles are illustrated in Figs. 8 and 9, respectively. Fig. 8 shows the time-domain waveforms of the 1st to 4th scattered echoes. It can be observed that under the influence of different scattering times, the echo signal exhibits a certain broadening phenomenon; Moreover, the more scattering times, the more obvious the broadening of the echo signal. In Fig. 9, from a time-domain perspective, when scattering times are 1 to 4, the widths of the echo signal after broadening are 4 ns, 14 ns, 22 ns and 26 ns, respectively. The results indicate that the width of the echo signal approximately linearly increases with the scattering times.

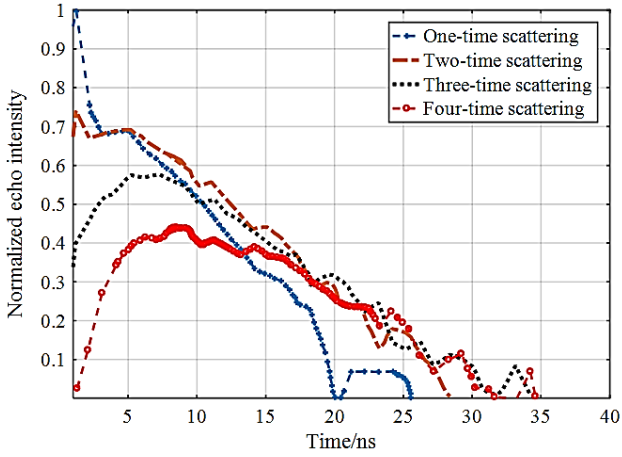


Fig. 8. The time-domain waveform of the same-order scattering echo in the backscattered echo (color online)

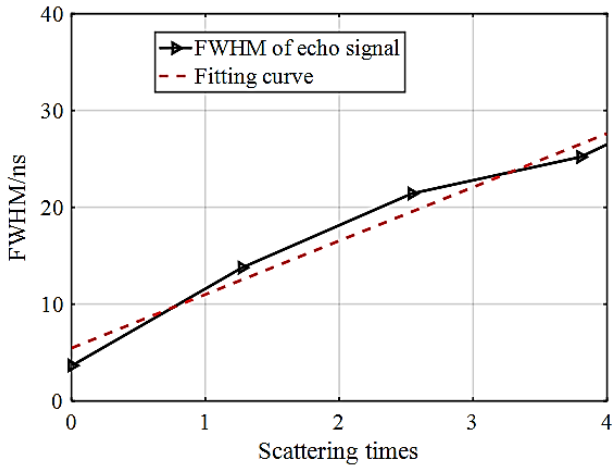


Fig. 9. Time-domain width curve of same-order scattered echoes in backscattered echo (color online)

To validate the correctness of the theoretical model established in this paper, a laser detection system for a certain type of laser fuse was used for static testing at different detection distances. The maximum value of the output signal of the system was 5 V. When the system detects a signal peak of 5 V, it indicates that the detection distance is relatively close, and the photoelectric receiver detects a higher target echo power, causing the photoelectric receiver to saturate. Tests were conducted at different detection distances of 5.5 m, 8 m, and 10 m, and the target echo signals under different detection distance conditions are shown in Figs. 10-12.

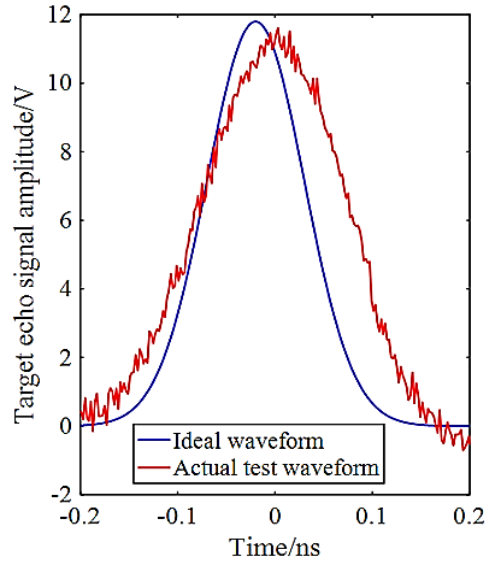


Fig. 10. The target echo signals at the detection distance of 5.5 m (color online)

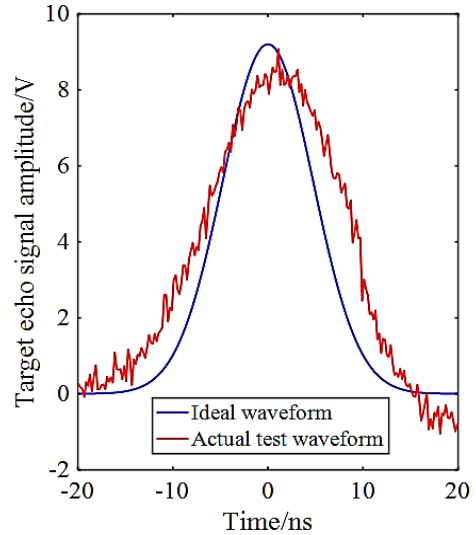


Fig. 11. The target echo signals at the detection distance of 8 m (color online)

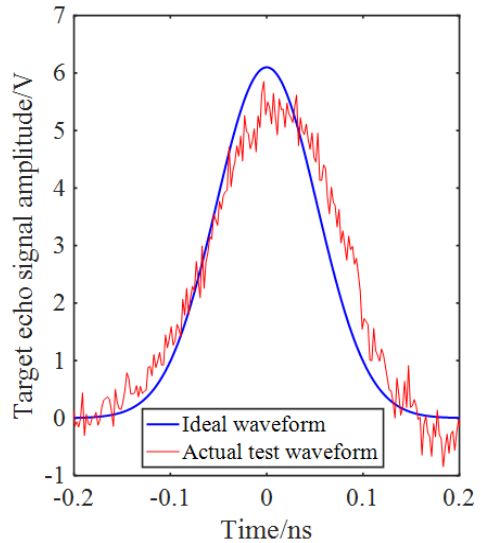


Fig. 12. The target echo signals at the detection distance of 10 m (color online)

It can be seen from the experimental test results that the obtained target echo waveform of the system closely resembles the theoretical results. When the detection distance is 5.5 m, the rising edge of the target echo signal is relatively consistent with the ideal signal, but the falling edge has some deviation from the ideal signal. This discrepancy is due to the proximity of the detection distance, resulting in a relatively high target echo power. And the echo signal sensed by the photoelectric receiver is relatively strong, resulting in a more saturated output of the photoelectric receiver. As the detection distance increases, the amplitude of the system's output target echo signal gradually decreases, but the degree of match between the target echo signal and the ideal signal is good. Since the laser fuse detection system adopts the threshold detection method, the deviation of the falling edge does not affect the determination of the test under threshold conditions.

6. Conclusions

The mathematical model of the received echo power of ground targets by the laser fuse detection system in complex atmospheric environments was established based on the Mie scattering theory, incorporating factors such as the transmission time and frequency of backscattered photons from the smoke particles, the photon weight after collision with the smoke particle, and others. Different particle backscattering characteristics were simulated and studied under various conditions, including pulse widths, mass concentration of smoke particles, and missile-target intersection distance. The findings indicate: (1) in the presence and absence of targets in suspended smoke particles environment, the echo waveform exhibited asymmetry. A narrower pulse width results in more pronounced asymmetry, making it easier to distinguish ground target echoes; (2) with a constant mass concentration of smoke particles, the echo intensity was inversely proportional to the missile-target intersection distance, the farther the missile-target intersection distance. The smaller the echo intensity, with lower mass concentrations of smoke particles leading to a gradual reduction in echo intensity; (3) the total number of smoke particle backscattering echoes was directly proportional to the mass concentration of smoke particles and inversely proportional to the missile-target intersection distance. The research provides a theoretical basis for exploring methods to enhance the detection performance of laser fuse in complex environments, with important theoretical significance and practical value. In addition, in rain and snow, the particle form is much larger than the particles suspended in the air in haze days, or soot particles, so that rain and snow have a great impact on laser detection, which is easy to cause the false trigger of laser fuse, mainly because the appearance of rain or snow is easy to form false echo signals before the detection of the target. The future research direction should focus on the anti-jamming method of laser in rain and snow weather, so as to further improve the detection performance of laser

fuse in harsh environment.

Acknowledgement

The research content of this paper comes from my research project of the Key Science and Technology Program of Shaanxi Province (No.2023-YBGY-341) and the National Natural Science Foundation of China (No.62001365).

References

- [1] Wei Zhang, Yinlin Li, Zhonghua Huang, Chao Ma, *Optik* **131**, 188 (2017).
- [2] Huimin Chen, Yang Liu, Xiongwei Zhu, Fengjie Wang, *Acta Armamentarii* **36**(12), 2247 (2015).
- [3] Shaoyu Xie, Yiqiang Zhao, Jinhua Wang, Xiaodong Jia, *Infrared and Laser Engineering* **46**(4), 49 (2017).
- [4] Zhengping Xu, Honghai Shen, Yongshen Xu, *Chinese Optics* **8**(1), 28 (2015).
- [5] Hanshan Li, Xiaoqian Zhang, Xuewei Zhang, Quanmin Guo, *Defence Technology* **18**(8), 1405 (2022).
- [6] Jingguo Zhang, Xiaogeng Liang, Jianxin Liu, Qingpo Niu, Jun Tang, *Acta Photonica Sinica* **41**(12), 1422 (2012).
- [7] Xueping Song, Feng Liu, Yifan Qin, *Infrared and Laser Engineering* **36**, 432 (2007).
- [8] Fengjie Wang, Huimin Chen, Changping Lu, *Guidance and Fuze* **40**(2), 22 (2019).
- [9] C. Hauger, E. Baigar, W. Zinth, *Optics Communications* **133**(1), 72 (1997).
- [10] Chenglin He, Qian Liang, *Aero Weaponry* **48**(1), 57 (2013).
- [11] Ying Liu, Ning Lv, *Laser and Infrared* **45**(9), 1028 (2015).
- [12] Huimin Chen, Xinyang Liu, *Optics and Precision Engineering* **23**(3), 626 (2015).
- [13] Haojun Zhang, Jianlin Zhao, *Infrared and Laser Engineering* **40**(6), 1070 (2011).
- [14] Hanshan Li, Xiaoqian Zhang, *IEEE Transactions on Instrumentation and Measurement* **71**, 7000111 (2022).
- [15] Chun Fu, Xi Pan, Chengtian Song, *Journal of Terahertz Science and Electronic Information Technology* **14**(1), 40 (2016).
- [16] Fengjie Wang, Huimin Chen, Chao Ma, Yinyu Long, *Infrared and Laser Engineering* **47**(5), 103 (2018).
- [17] Qingcai Chen, Mamin Wang, Yuqin Wang, Lixin Zhang, Yanguang Li, Yuemei Han, *Environmental Science and Technology* **53**(15), 8574 (2019).
- [18] Honglei Wang, Yue Ke, Yue Tan, Bin Zhu, Tianliang Zhao, Yan Yin, *Chemosphere* **327**, 138548 (2023).
- [19] Yue Tan, Honglei Wang, Bin Zhu, Tianliang Zhao, Shuangshuang Shi, Ankang Liu, Duanyang Liu, Chen Pan, Lu Cao, *Environmental Research* **214**, 114095 (2022).

- [20] Xin Huang, Ke Ding, Jingyi Liu, Zilin Wang, Rong Tang, Lian Xue, Haikun Wang, Qiang Zhang, ZheMin Tan, Congbin Fu, Steven J. Davis, Meinrat O. Andreae, Aijun Ding, *Science* **379**(6631), 457 (2023).
- [21] Hanshan Li, Xiaoqian Zhang, *Defence Technology* **19**(1), 63 (2023).
- [22] Bingting Zha, Zhen Zheng, Haojie Li, Guangsong Chen, Hailu Yuan, *Optik* **247**, 168020 (2021).
- [23] Zhiyong Shi, Xiaosheng Pan, Qian Zhang, *Optics and Precision Engineering* **22**(2), 252 (2014).
- [24] Fengjie Wang, Huimin Chen, *Optics and Precision Engineering* **23**(10), 1 (2015).
- [25] Saverio Mori, Frank S Marzano, *Applied Optics* **54**(22), 6787 (2015).
- [26] Hanshan Li, Xiaoqian Zhang, Xuwei Zhang, Quanmin Guo, *Defence Technology* **18**(8), 1405 (2022).
- [27] Wei Zhang, Yinlin Li, Zhonghua Huang, *Optik* **127**(20), 9046 (2016).
- [28] Xiaoqian Zhang, Hanshan Li, Junchai Gao, *Applied Optics* **60**(24), 7437 (2021).
- [29] Liping Lu, Hanshan Li, *Microwave and Optical Technology Letters* **62**(12), 3811 (2020).
- [30] Zeyu Zhang, Xiaoping Xie, Tao Duan, Yu Wen, Wei Wang, *Infrared and Laser Engineering* **45**, 42 (2016).
- [31] Hanshan Li, *Microwave and Optical Technology Letters* **65**(1), 356 (2022).
- [32] Xiaoqian Zhang, Hanshan Li, *Microwave and Optical Technology Letters* **62**(7), 2463 (2020).
- [33] Hanshan Li, Xiaoqian Zhang, Junchai Gao, *IEEE Sensors Journal* **22**(22), 21600 (2022).
- [34] Huimin Chen, Chao Ma, Bin Qi, Pengyu Guo, Shangxian Yang, Lijuan Gao, Jian Huo, *Infrared and Laser Engineering* **49**(4), 0304005 (2020).
- [35] Fengjie Wang, Ximin Liu, Changping Lu, *Infrared and Laser Engineering* **49**(4), 0403006 (2020).
- [36] Liping Lu, Hanshan Li, *Microwave and Optical Technology Letters* **62**(12), 3811 (2020).

*Corresponding author: xiaoqianzh1983@yeah.net